Preliminary Pulsed MPD Thruster Performance

Matthew T. Domonkos and Alec D. Gallimore
Plasmadynamics and Electric Propulsion Laboratory
The University of Michigan
Ann Arbor, MI 48109

Roger M. Myers
NYMA Inc.
NASA Lewis Research Center
Brookpark, OH 44142

Erica Thompson
Fisk University
Nashville, TN 37208

Abstract
A thrust stand was modified, and a primary calibration technique was developed to evaluate the performance of applied-field pulsed magnetoplasmadynamic thrusters (MPDTs) for 10 kW class solar electric orbit transfer vehicle (SEOTV) missions. The NASA Lewis Research Center (LeRC) 30 kW thrust stand was modified to accept high current pulses delivered to the MPDT. A pendulum system was developed to deliver an in situ primary impulse calibration of the thrust stand. An MPDT was built to accommodate future testing of an externally heated cathode and to allow rapid diffusion of the applied magnetic field. The thruster was driven by a pulse forming network to anode-cathode powers of 350 kW. The thrust stand was calibrated for impulses ranging from 4.8 to 12.2 mN-s, and thruster discharges generated impulses ranging from 2.6 to 4.5 mN-s after subtracting the cold gas flow impulse.

Nomenclature

E_p	=pulse energy, J
g_o	=9.81 m/s^2
I	=impulse bit, N-s
I_{sp}	=specific impulse, s
m	=mass, kg
$\acute{m}$	=mass flow rate, kg/s
$\bar{v}$	=velocity, m/s
η	=thruster efficiency
τ_p	=pulse time, s

Introduction

Performance data and recent systems studies have shown that the use of 10 kW class pulsed applied-field magnetoplasmadynamic thrusters (MPDTs) for primary satellite propulsion may reduce launch costs for spacecraft more than 1000 kg in mass.[1-3] Extrapolation of power level trends for communications satellites indicates that next generation satellites can be expected to have power generation in excess of 10 kW, and could cut launch costs through the use of primary electric propulsion.[4] Pulsed MPDTs are effectively 10 kW class gas-fed pulsed plasma thrusters (PPTs) since they make use of similar acceleration mechanisms and nearly identical operation philosophies. Each type of thruster is designed for a uniform pulse, and power scaling is accomplished by adjustment of the duty cycle. While PPTs have been flight tested on the LES 6, LES 8/9, and NOVA spacecraft, Japanese researchers have space tested three pulsed MPDT systems including the Electric Propulsion Experiment (EPEX) currently in orbit on the Space Flyer Unit (SFU).[5-11] The demonstrated capability and renewed interest in PPTs may serve to bring a spotlight on the benefits of pulsed thrusters. However, performance measurements of a thruster closely approximating the type necessary for primary propulsion must justify further development of pulsed MPDTs. The purpose of this work was to develop a system capable of accurate performance measurements of a pulsed MPDT in order to facilitate testing of a thruster designed to meet orbit transfer requirements.

MPDT development in the U.S. has focused primarily on high power (>100 kW) steady-state thrusters with quasi-steady pulsed operation being investigated in the absence of facilities capable of handling the large heat and propellant fluxes of high power thrusters.[12,13] Efforts to date have shown the benefits of high power operation and the use of applied magnetic fields.[13] Japanese researchers have developed the pulsed MPDT as a propulsion system capable of operation over a wide range of input power, and pulsed applied-field thruster efficiencies in excess of 50 percent using hydrogen and

as high as 25 percent on ammonia have been reported.[2,14] Pulsed operation greatly facilitates scaling of the thruster to different power levels since a change in available power can be accommodated by a corresponding alteration of the pulse frequency without any loss in thruster efficiency.[1] Consequently a single thruster design would be sufficient over a great range of power levels.[1,15] Further, testing facility requirements are less stringent compared with steady state thrusters since performance can be evaluated on a single shot basis. This eliminates the need for a high pumping speed testing facility with thermal management capabilities. Both of these properties would reduce the development costs of pulsed MPDTs.

Pulsed MPDT system design must address the issues of component lifetime, applied-field diffusion into the discharge, propellant injection and utilization, and pulse forming network (PFN) design.[1,15,16] The component lifetime required for orbit transfer remains undemonstrated.[12,17] Cathode lifetime, which is limited to 100 to 200 hours under cold cathode operation, would be extended by the use of an externally heated low work function cathode, and recent works have attempted to incorporate thermionically emitting cathodes into pulsed MPDTs.[17.18] Applied-field diffusion into the discharge chamber can be accomplished by placing axial slits in the anode.[19] While diffusion experiments in the absence of a plasma indicated that two slits were sufficient, discharge data are necessary to draw a final conclusion.[15] The union of these components may be necessary for a pulsed MPDT to fulfill primary propulsion requirements.

This paper presents the preliminary results of an effort to develop a pulsed MPDT thrust stand and to measure the performance of a thruster designed to meet the needs for orbit transfer. The work included modification of the NASA Lewis Research Center (LeRC) 30 kW thrust stand, and construction of the pulse forming network (PFN) and thruster. Since the thrust stand and thruster were the centerpieces of this work, the apparatus used in this investigation are described in detail. The experimental procedure is then discussed, followed by the preliminary results. Analyses of both the thrust stand operation and the initial thruster tests are presented, and finally, a summary of the conclusions is included.

Experimental Apparatus
Since the primary focus of this work was to develop a technique to make accurate performance measurements of a pulsed MPDT, thrust stand construction, operation, and calibration comprised the bulk of the effort. The thruster and PFN were designed to meet many of the requirements of a 10 kW class solar electric orbit transfer vehicle (SEOTV).

Thrust Measurement
The NASA LeRC 30 kW arcjet thrust stand, shown in Figure 1a, was modified to handle the high pulsed currents supplied to the thruster.[20] The thrust stand is a displacement type based on an inverted ballistic pendulum. The power flexures consisted of two 0.6 cm diameter copper tubes. These were tightly tied together at the corners and loosely held at the midpoint of the large spans of the flexure. This prevented the flexures from separating from each other during current flow and acting as a nonlinear spring. The natural spring constant of the thrust stand was sufficient to restrict the motion to a small range, thus, an additional spring was omitted. Voltage signals and the valve supply were carried through internal flexures, while the instrument lead to the piezoelectric pressure transducer on the thruster was strung to add minimal resistance to motion. Since thermal loads to the thrust stand were expected to be negligible, the water cooled shroud was removed during testing to facilitate thrust stand inspection and adjustment. Instrument signal quality was not compromised by the absence of the shroud.

1a) Thrust Stand Modification
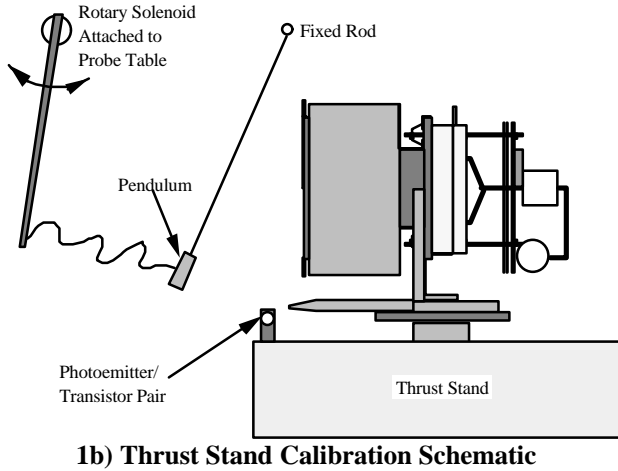
1b) Thrust Stand Calibration Schematic

Fig. 1 - Thrust Stand Apparatus

The deflection of the thrust stand was measured using a Schaevitz HR 100 Linear Voltage Differential Transformer (LVDT) connected to a Schaevitz DTR 451 primary supply and readout. The output of the readout was sent through a low pass filter to the oscilloscope. Oscilloscope traces were used to determine the maximum displacement of the thrust stand as a function of impulse.

Impulse could be determined using the initial velocity of the thrust stand and multiplying it by the mass in motion. However, LVDT signal noise prevented this approach. For small deflections, the maximum deflection of the thrust stand was linearly proportional to the delivered impulse, and this was the basis for impulse calibration and measurement. The thrust stand was calibrated for impulses ranging from 4.8 to 12.2 mN-s using a cylindrical pendulum as shown in Figure 1. Equation 1 defined the pendulum impulse, I, as

$$I = m\left(\overline{v}_{in} - \overline{v}_{out}\right). \qquad (1)$$

The system was designed to permit remote operation and allowed calibration under vacuum. The pendulum had a mass of 7.04 g and was suspended by a 0.2 mm diameter plastic filament. A rotary solenoid with a rigid arm attached was positioned at several different distances from the thruster by a probe positioning table. The rotary solenoid was used to retract the pendulum, and the pendulum was released when the solenoid was deenergized. The period of the arm-solenoid combination was shorter than that of the pendulum to ensure that the connecting line was slack throughout the swing of the pendulum. The voltage across the phototransistor increased when the pendulum interrupted the signal from the photoemitter, and was recorded on an oscilloscope. The effective diameter of the pendulum for blocking the transistor

from the emitter measured 9.9 mm. The pendulum impacted a bar 14 cm below the cathode of the thruster. Since the thrust stand has planar motion, deflections caused by the pendulum and by the thruster were related with a unit scale factor.

Thruster
Preliminary tests were performed on the NASA Lewis thruster shown in Figure 2. The design was chosen to be robust, and to facilitate incorporation of a heated low work function cathode. The cold cathode used for preliminary tests was made to similar dimensions and of the same material as the heated cathodes. This ensured that performance measurements with the cold cathode could be compared directly with those of the heated cathode. The copper anode was flared with a 6.4 cm diameter by 2.5 cm long cylindrical throat that diverged conically to an 11.4 cm diameter exit through a 16° half angle. The throat facilitated discharge initiation at voltages as low as 500 V. The applied-field magnet consisted of a single turn of copper sheet 7.6 cm long with a 15.2 cm diameter. The magnet generated an estimated cathode tip field strength of 825 G at 5000 A. The anode was slitted axially in two places to permit rapid diffusion of the applied-field.[15] Ceramic cement was used to fill the slits thereby preventing propellant leakage through the sides.
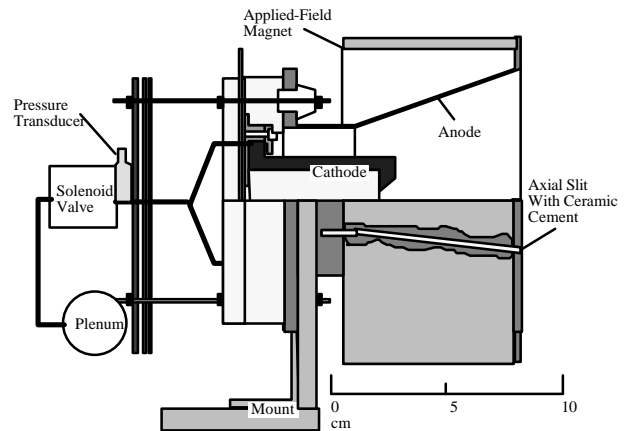

Fig. 2 - Thruster Schematic

The propellant injection design initially focused solely on obtaining a quasi-steady flat-top gas pulse, however, subsequent designs will attempt to reduce the duration of the gas pulse. Quasi-steady operation was obtained by ensuring that the sonic orifice was as close to the discharge chamber as possible. The mass flow rate was calibrated by closing off the plenum, pulsing the valve, and observing both the pressure drop in the plenum and the transient pressure downstream of the valve. From this, the orifice area multiplied by the discharge coefficient based on one dimensional isentropic flow was 2×10^{-7} m^2. A 15 μF capacitor was

used to open the valve, however, a smaller capacitor could be used to reduce the pulse duration provided the energy storage remains high enough to open the valve. A ceramic propellant isolator insulated the valve from the cathode.

Pulse Forming Network

The University of Michigan pulse forming network (PFN), shown schematically in Figure 3, drove the arc discharges. The PFN design was motivated by the results of the systems study by Myers, et al., which suggests that the pulse duration should be short to minimize the PFN energy storage and mass, but also of sufficient length to utilize a large fraction of the injected propellant.[1] The second constraint forced the pulse time to be greater than 1 ms in order to use existing valve technology. The PFN consisted of ten stages of capacitors with a maximum energy storage capacity of 4 kJ at 1000 V, and a characteristic pulse time of 2 ms. An International Rectifier 2000V, 45000A surge silicon controlled rectifier (SCR) was used for high current switching. The SCR was controlled through a firing board which was triggered by a signal from a B&K Pulse Generator. The SCR firing signal was delayed 3 to 10 ms so that the gas pulse could be considered quasi-steady during the discharge. Number 2 cable electrically connected the PFN to the thrust stand. The discharge current was measured using a Rogowski coil, which was calibrated by discharging the PFN through a 1 mΩ shunt with calibrated voltage probes measuring the potential.
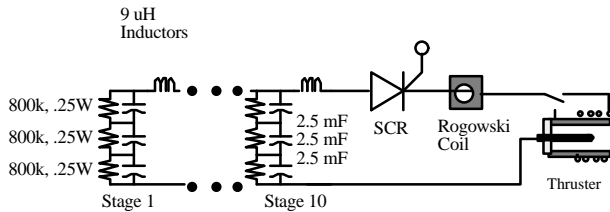

Fig. 3 - PFN Circuit Diagram

Vacuum Facility

Tests of the thrust stand and preliminary thruster firings were conducted in the University of Michigan 9 m by 6 m diameter vacuum chamber, shown schematically in Figure 4. The chamber was pumped by six 0.81 m diameter oil diffusion pumps which were backed by two mechanical blowers and four mechanical pumps. A Polycold system over two of the diffusion pumps removed water vapor from the tank atmosphere. The diffusion pumps provided a pumping speed of about 300000 L/s of hydrogen. Two ion gages measured the tank pressure during testing. The facility base pressure was 2.7×10^{-3} Pa. A leak of approximately 3 mg/s, measured by an MKS flow controller, in the gas pulse valve caused the facility

pressure to be 9.3×10^{-3} Pa during testing. The thrust stand was located on the thruster station shown in Figure 4, which placed the thruster axis approximately coincident with the chamber axis, minimizing the effects of facility interference.
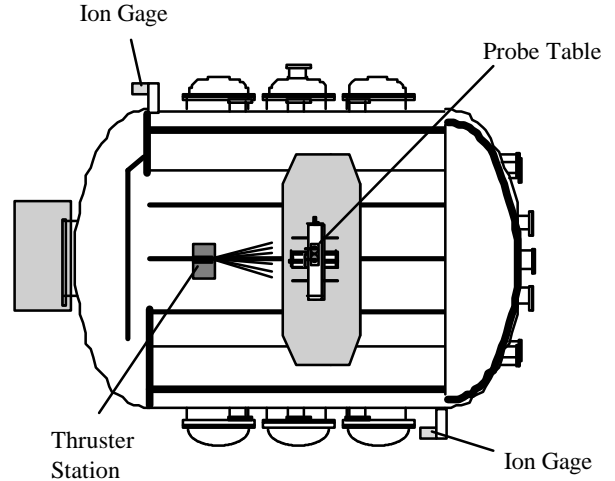

Fig. 4 - The University of Michigan Vacuum Chamber

Data acquisition was accomplished using a Tektronix TDS 540 digital oscilloscope connected to a Macintosh IIci computer equipped with the LabVIEW data acquisition hardware and software. Tektronix 1000:1 voltage probes, connected differentially to a Tektronix 501 operational amplifier, were used to measure the discharge voltage of the thruster. The output voltage signal was sent to the oscilloscope. The probes were calibrated against a Fluke 77 digital multimeter. Pressure measurements in the propellant plenum were made using an Omega PX425 absolute pressure transducer connected to a digital process readout. The sensor was calibrated against a laboratory standard transducer, and showed linearity up to 310 kPa. A Piezotronics 112A21/62 piezoelectric pressure transducer measured the transient gas pulse in the propellant injection line. The signal was sent to a charge amplifier which produced a voltage output for the oscilloscope. The transducer resolution was 14 Pa.

Experimental Procedure

Tares due to high current operation and cold gas flow were evaluated to establish their contribution to the impulse measured from the thruster discharge. Initially, tests were conducted under atmospheric conditions to evaluate the magnitude of the thrust stand oscillations generated by pulsing up to 6 kA through the thrust stand and the applied-field magnet alone. The tests showed that the single turn magnet generated no discernible thrust impulse at current levels up to 6 kA. The thrust stand exhibited a zero offset after each

thruster discharge, and analysis of the LVDT signal indicated that the offset was generated during and within a few milliseconds following the current pulse. The voltage corresponding to the offset was evaluated by averaging the LVDT signal when resolvable thrust stand oscillations ceased. Thrust stand deflection from a cold gas pulse was also calibrated; performance calculations include only the fraction of the cold gas flow during the discharge.

Pendulum calibrations were conducted both at atmosphere and again under vacuum just prior to testing. Direct calibration eliminated the need to determine a spring constant for the thrust stand.[21] After the first impact of the pendulum, the rotary solenoid was energized again to prevent a second impact. Typical output from the phototransistor appears in Figure 5. The velocity of the pendulum was calculated as the effective diameter divided by the time that the voltage remained at its peak. The delivered impulse was calculated as the mass of the pendulum multiplied by the change in velocity. The probe tables moved the solenoid to provide various impulses and were also used to remove the pendulum to a position away from the discharge during testing.
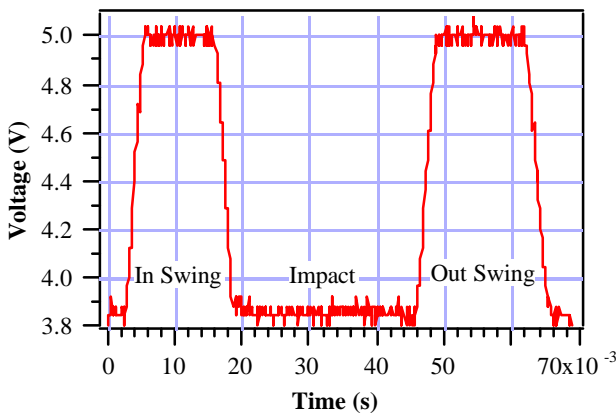

Fig. 5 - Phototransistor Response to Pendulum Passage

The NASA LeRC thruster was operated on hydrogen to test the calibration technique. The thrust stand was operated without a damper in order to eliminate any potential offsets created by the restriction of motion caused by the damper. An offset would corrupt the thrust measurement since any amount of potential energy stored in the thrust stand would be converted to velocity when the damper was released.

Results and Discussion

Calibrations performed in atmosphere and under vacuum differed somewhat as shown in Figure 6, and this result illustrates the need for in situ calibration.

These data were taken immediately prior to testing the thruster. The difference in the signals was attributed to warping of the chamber under vacuum which displaced the elements of the calibration system and thrust stand a small amount. Since the cylindrical pendulum could develop angular motion after an impact if improperly aligned, care was taken in evaluating the validity of the vacuum calibration. Video taped images of the impact and deviation of the phototransistor voltage signal from that in Figure 5 were indications of misalignment and thus invalid pendulum impulses. The calibration in Figure 6 shows the expected linear response of the thrust stand. Since only two points were obtained under vacuum, the performance calculations reported here were based on the linear curve fit to the atmospheric data. Additional tests of the pendulum showed a similar trend with the slope of the vacuum data approximately 10 percent smaller than the atmospheric tests. Consequently the performance estimates reported here are conservative.

Figures 7 compare the LVDT output during two calibration tests (a,b) and an arc discharge (c). The zero offset has been removed from each of these plots to facilitate comparison. These data show that the period of the thrust stand was approximately 1.6 seconds. The calibration signals appeared relatively free of noise
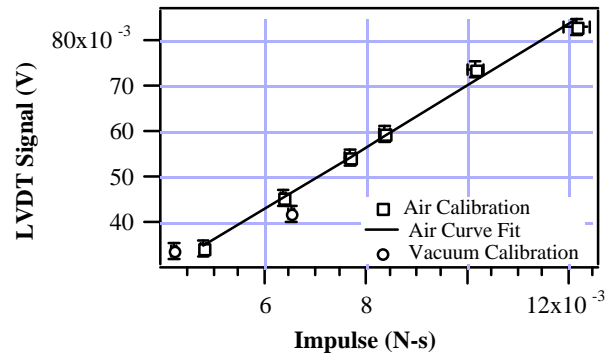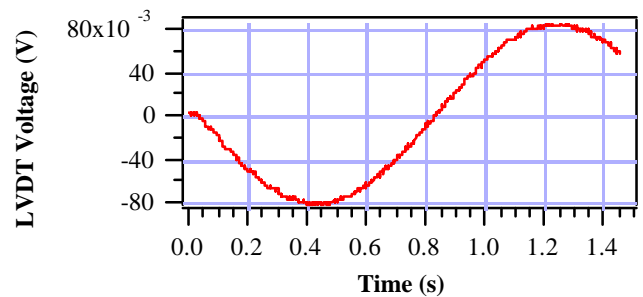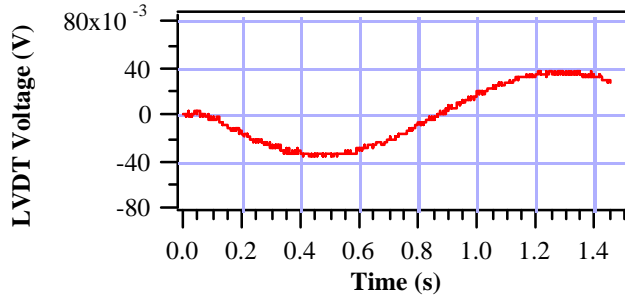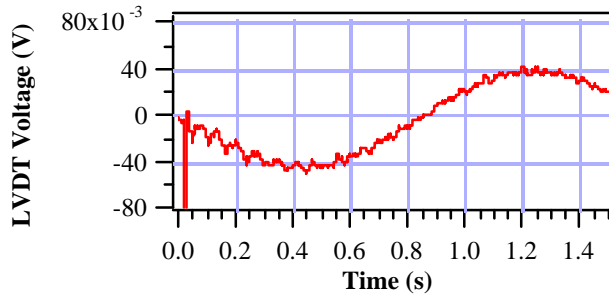

Fig. 6 - Calibration Showing Two Valid Vacuum Impulses

7a) 12.2 mN-s Pendulum Calibration

5

7b) 4.8 mN-s Pendulum Calibration

7c) 4.2 mN-s Impulse from the Thruster Discharge

Fig 7 - Impulse Responses

or harmonics from the thrust stand. However the signals generated from the thruster pulse showed considerably more noise, including the initial spike during the discharge. The harmonics in the LVDT responses were reproducible. The maximum displacement was taken as the average of the values between 0.4 and 0.5 seconds after the discharge in order to minimize the perturbation due to random noise.

Preliminary Thruster Tests
Typical propellant pulses appear in Figure 8. The flat-top duration of the pressure transducer signal was 10 ms long and the tail was attributed to both the valve closing time and the small ratio of the orifice area to the volume between the valve and the orifice. The mass flow rate was integrated over the pulse to yield the total pulse mass. Since pulsed system mission design relies on the impulse per pulse, mass flow per pulse, and pulse energy in order to evaluate system viability, these quantities are reported.
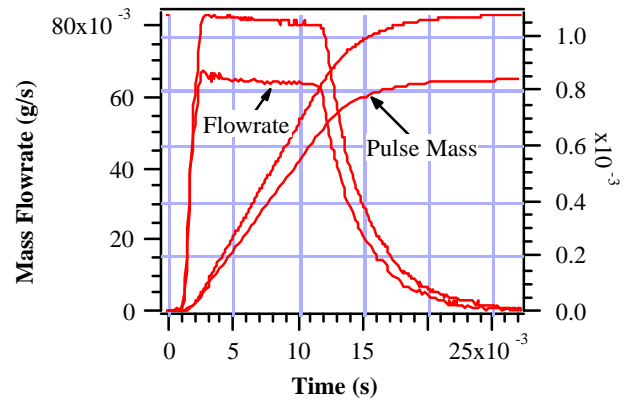

Fig. 8 - Typical Gas Pulses

Figures 9a-c illustrate typical gas, current and voltage pulses. The propellant pulses appeared to be very similar to the ones shown in Figure 8. The notable exception was the spike that occurred during the thruster discharge. Since the transducer is a piezoelectric device, the spike was attributed to noise pick up during the discharge. Consequently, the pulse flow rate was based on the quasi-steady value. The current pulse in Figure 9b represents a typical shot with a length of ~2 ms. Using these data and that in Figure 8, 85 percent by mass of the gas pulse was cold flow.

The use of an SCR for switching allowed the full PFN voltage to be applied across the anode-cathode gap prior to opening of the SCR. Once the propellant was injected, the hydrogen was ionized, and the voltage dropped to the value necessary to carry the leakage current of the SCR. After the SCR was triggered the voltage dropped again to the arc value. Some ringing was observed following the pulse.
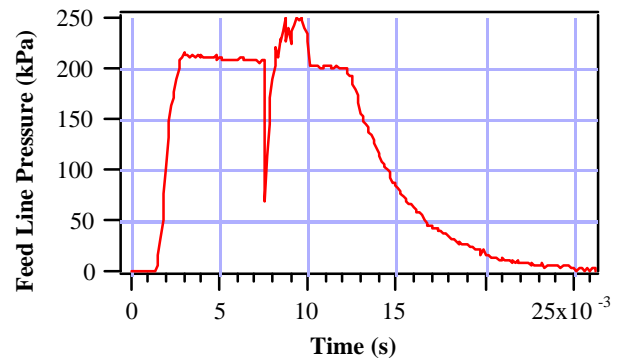

9a) Propellant Injection Pulse
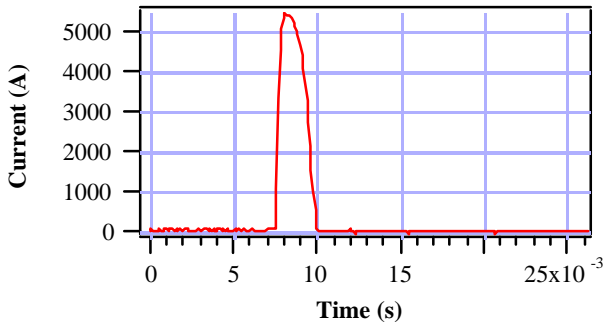
9b) Discharge Current Pulse
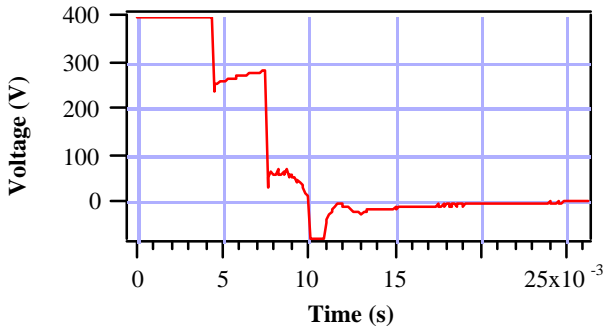
9c) Anode-Cathode Voltage Trace Showing Structure Prior to the Current Pulse

The pulse power and energy appear in Figure 9d. Only the anode-cathode power is reported, since tests determined that the magnet consumed less than five percent of the discharge power. The pulse energy was calculated by simply integrating the pulse power over time and treating the non-zero energy at the beginning of the pulse as a numerical defect. The pulse energy failed to match the PFN energy largely due to line
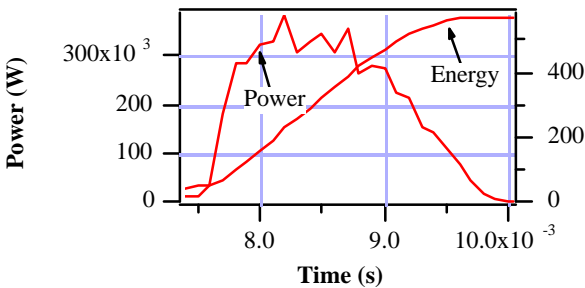
9d) Pulse Power and Energy

Fig. 9 - Thruster Pulse Characteristics

losses since the PFN and thruster were separated by approximately 9 m.

Data were obtained at mass flow rates of 0.065 g/s and 0.083 g/s. Impulses ranged from 2.6 to 4.5 mN-s. The results are summarized in Figure 10. The specific impulse was calculated using Equation 2,

$$I_{sp} = \frac{I}{g_o \dot{m} \tau_p} \qquad (2)$$

and Equation 3 defined the efficiency

$$\eta = \frac{I g_o I_{sp}}{2 E_p} . \qquad (3)$$

The data show the general positive trend between specific impulse and efficiency. Since the primary goal of this work was to establish a means to accurately measure pulsed MPDT thrust and little effort was made to vary thruster operating characteristics or optimize the thruster design, further conclusions concerning thruster performance are left to future work.
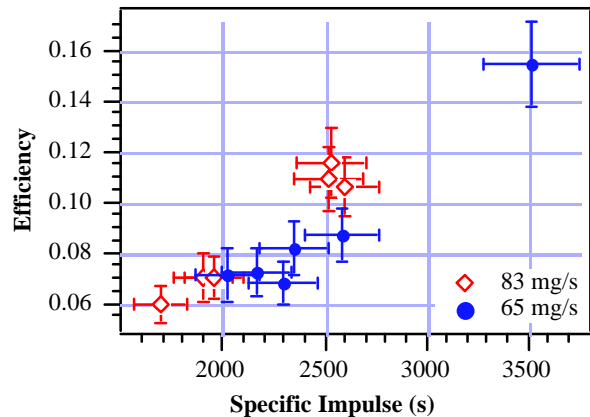

Fig. 10 - Preliminary Performance Trends

Conclusions

The NASA LeRC 30 kW thrust stand was modified to test pulsed MPDTs, and an in situ primary calibration system was used. A remotely operated pendulum provided a direct impulse calibration of the thrust stand under vacuum. A phototransistor-diode pair was used to determine the pendulum velocity before and after the impact. The pendulum calibration spanned the range of impulses delivered by the thruster.

A thruster was built to incorporate both a heated low work function cathode and applied magnetic field diffusion into the discharge chamber. A pulse forming network was constructed to drive the thruster and to meet some of the requirements for SEOTV system design. Preliminary tests of the thruster on the thrust stand were performed in the University of Michigan vacuum facility. These tests indicated specific impulses of 1700 to 3500 s with impulse bits between 2.6 and 4.5 mN-s. Further research is necessary to establish the range of performance of this thruster, and operation with storable propellants and a low work function heated cathode must be characterized to establish a basis for continued development.

7

References

1.   Myers, R.M., Domonkos, M., and Gilland, J.H., "Low Power Pulsed MPD Thruster System Analysis and Applications," AIAA Paper 93-2391, Monterey, CA, June 1993.

2.   Tahara, H., Sasaki, M., Kagaya, Y., and Yoshikawa, T., "Thruster Performance and Acceleration Mechanisms of a Quasi-steady Applied-field MPD Arcjet," AIAA Paper 90-2554, Orlando, FL, July 1990.

3.   Myers, R.M., "Applied-Field MPD Thruster Performance with Hydrogen and Argon Propellants," *Journal of Propulsion and Power*, Vol. 9, No. 5, Sept.-Oct. 1993, pp. 781-784.

4.   *Janes Space Directory, 10th Edition 1994-95*, Ed. by Wilson, A., Biddles Ltd., Guildford and King's Lynn, Great Britain, pp. 303-305, 333-335.

5.   Vondra, R.J. and Thomassen, K.I., "Flight Qualified Pulsed Electric Thruster for Satellite Control," *Journal of Spacecraft and Rockets,* Vol. 11, No. 9, Sept. 1974, pp. 613 - 617.

6.   Brill, Y., Eisner, A., and Osborn, L., "The Flight Application of a Pulsed Plasma Microthruster; The Nova Satellite," AIAA Paper 82-1956, November 1982.

7.   Kuriki, K., Morimoto, S., Nakamura, K., "Flight Performance Test of MPD Thruster System," AIAA Paper 81-0664, April 1981.

8.   Kuriki, K., "The MPD Thruster Test on the Space Shuttle," *Journal of Spacecraft and Rockets*, Vol. 16, No. 5, September-October 1979, pp. 326-332.

9.   Kuriki, K., Nakamura, K., and Morimoto, S., "MPD Thruster Test on Engineering Test Satellite," AIAA Paper 79-2071, Oct. 1979.

10.   Sazaki, S., et al., "Neutralization of Beam-Emitting Spacecraft by Plasma Injection," *Journal of Spacecraft and Rockets*, Vol. 24, No. 3, May - June 1987, pp. 227-231.

11.   Shimizu, Y., Toki, K., Suzuki, H., Uematsu, K., Ostuka, T., Shiina, K., and Kunii, Y., "Development of MPD Arcjet System EM for SFU-1," IEPC Paper 91-147, *Proceedings of the 22nd International Electric Propulsion Conference,* Viarregio, Italy, Oct. 1991.

12.   Mantenieks, M.A. and Myers, R.M., "100-kW Class Applied-Field MPD Thruster Component Wear," 10th Symp. on Space Nuclear Power and Propulsion, *AIP Proceedings No. 271*, Jan. 1993, pp. 1317-1326, see also NASA TM - 106023.

13.   Myers, R.M., Mantenieks, M.A., and LaPointe, M.R., "MPD Thruster Technology," AIAA Paper 91-3568, Cleveland, OH, Sept. 1991.

14.   Kuriki, K., Shimizu, Y., Morimoto, S., Kuwahara, K., Kisarage, T., Uematsu, K., Enya, S., and Sasao, Y., "MPD Arcjet System Performance Test," *Acta Astronautica*, Vol. 12, No. 6, pp. 391-403, 1985.

15.   Domonkos, M.T., Roderick, N.F., and Myers, R.M., "10 kW Class Pulsed MPD Thruster Design," AIAA Paper No. 94-2992, Indianapolis, IN, June 1994.

16.   Rudolph, L.K., "Design and Benefits of Pulsed MPD Thruster Orbit Transfer Vehicles," IEPC Paper 84-81, pp. 590-599.

17.   Myers, R.M., Domonkos, M., and Gallimore, A., "Evaluation of Externally Heated Pulsed MPD Thruster Cathodes," IEPC Paper 93-116, Seattle, WA, Sept. 1993.

18.   Andrenucci, M., Paganucci, F., and La Motta, G., "MPD Thruster Performance with Cathode Heating," AIAA Paper 92-3458, Nashville, TN, July 1992.

19.   Tahara, H., Kagaya, Y., and Yoshikawa, T., "Hybrid MPD Thruster with Axial and Cusp Magnetic Fields," IEPC Paper 88-058, *Proceedings of the 20th Internatinal Electric Propulsion Conference*, Garmisch-Partenkirchen, W. Germany, Oct. 1988, pp. 333-341.

20.   Haag, T.W., "Recent Testing of 30 kW Hydrogen Arcjet Thrusters," NASA TM 106214, AIAA Paper No. 93-1902, Monterey, CA, June-July, 1993.

21.   Haag, T.W., "PPT Thrust Stand," AIAA Paper No. 95-2917, San Diego, CA, July 1995.